Journal of Thermal Analysis and Calorimetry (2021) 143:899–913
https://doi.org/10.1007/s10973-020-09351-1

Impact of orientation and water depth on productivity of single-basin dual-slope solar still with Al_2O_3 and CuO nanoparticles

Kalpesh V. Modi[1] · **Hardik K. Jani**[2] · **Ilesh D. Gamit**[3]

Received: 21 November 2019 / Accepted: 13 January 2020 / Published online: 31 January 2020

Abstract
The thermal performance of solar still can be enhanced by means of nanoparticles. The core aim of the present work is to identify the influence of nanoparticles on productivity of single-basin dual-slope solar still through the experimental investigation with different glass cover orientations of still and the varying water depth in basin. Two identical single-basin dual-slope solar stills were fabricated, and experiments were conducted at location (20.61° N, 72.91° E). In first set of experiments, comparison of productivity of the still without nanoparticles and the still with 0.1% mass concentration of aluminium oxide (Al_2O_3) nanoparticles has been made at different depths of water. The experiments were conducted with glass covers oriented towards East–West and North–South directions. Compared to the still without nanoparticles, enhancement of 19.40%, 28.53% and 26.59% in distilled output was obtained with Al_2O_3 nanoparticles at the 30 mm, 20 mm and 10 mm water depth for the North–South orientation, respectively. The enhancement of 58.25% and 56.31% in yield was obtained for 20 mm and 10 mm water depth with copper oxide (CuO) nanoparticles for the North–South orientation. Compared to the still with 0.1% Al_2O_3 nanoparticles, 27.27% and 26.60% higher productivities were achieved at 20 mm and 10 mm water depths with the use of 0.1% CuO nanoparticles for the glass covers oriented towards North–South directions. Therefore, enhancement in thermal performance of single-basin dual-slope solar still was observed higher with the consumption of CuO nanoparticles than the Al_2O_3 nanoparticles.

Keywords Distillation · Heat storage · Heat transfer · Nanoparticles · Solar energy · Solar still

Introduction

Pure drinking water is an essential requirement for human beings. Origin and continuation of mankind is dependent on water. Water is abundantly available natural substance and covers around 71% of the earth's surface. About 97% water is available in the ocean as brackish water [1]. Only 3% of the quantity of available water is in the fresh and drinkable form [2]. Moreover, only less than 1% of the available potable water is in reach of human beings. The rest is in the form of permanent ice, snow cover and permafrost. The requirement of water continuously increases with the world population; hence, there is an urge of desalinate the brackish water to get potable water. Currently, the widely and most commonly used technique for the purification of water is reverse osmosis. Other techniques such as multi-effect distillation, vapour compression, multi-stage flash distillation and vacuum distillation are also utilized for water purification [3]. Solar desalination is an ingenious technology that utilizes the solar energy as an abundant and non-conventional energy source for distillation of brackish water [4]. The apparatus utilized for solar distillation is called as solar still. The solar still can also be utilized as regenerator for liquid desiccant [5].

Muftah et al. [6] have analysed the factors influencing the performance of solar still and deduced that the productivity depends upon the still body, its directional arrangement, water mass in basin, condensing cover angle and vapour tightness. Xiao et al. [7] have analysed the effect of environmental parameters on performance of still such as incident intensity of solar radiation, wind velocity around the solar

✉ Kalpesh V. Modi
kvmgecv@gmail.com

[1] Department of Mechanical Engineering, Government Engineering College, Bhuj, Gujarat 370001, India

[2] School of Technology, Pandit Deendayal Petroleum University, Gandhinagar, Gujarat 382007, India

[3] Department of Mechanical Engineering, Government Engineering College, Valsad, Gujarat 396001, India

still and ambient temperature. Further, water depth in basin, influence of temperature difference among basin water and glass cover, thermal insulating material and inclination of glass cover were also studied. The water evaporation rate in passive-type conventional solar still (CSS) relies upon the incident solar radiation and water depth in still basin. Previous experimental studies indicate that the quantity of distilled yield from CSS has inverse proportionality relation with basin water depth [8, 9]. Modi et al. [10] have carried out an experiment to analyse the influence of water depth (40 mm, 30 mm, 20 mm and 10 mm) on the yield of double-basin single-slope (DBSS) solar still. The 13% higher yield was achieved by authors at water depth of 10 mm than the 40 mm. Modi and Modi [11] have conducted an experiment on DBSS solar still having small piles of wick material (black cotton and jute cloth) to study the impact of water depth (20 mm and 10 mm) on yield. Compared to 20 mm water depth, higher yield of 9.81% and 13% was achieved at 10 mm water depth with wick pile of jute cloth and black cotton cloth, respectively. Jani and Modi [12] have studied the influence of water depth (30 mm, 20 mm and 10 mm) on the yield of single-basin dual-slope (SBDS) solar still with square and circular cross-sectional hollow fins. Compared to 20 mm water depth, higher yield of 17.51% and 3.32% was achieved at 10 mm water depth with circular fin and square fin, respectively. Modi et al. [13] have achieved the higher productivity with increase in water mass for spherical basin solar still integrated with parabolic concentrator.

The distillation through CSS has a lesser output [14]. Hence, the concept of dual-slope solar still was developed with the aim of boosting the performance of solar still [14]. Elango et al. [15] have concluded that the higher distilled yield was achieved for double-slope solar still as compared to the CSS. The performance of solar still can also be enhanced by the use of multi-slope glass cover solar still as it enhances the condensation area, receives higher solar radiation, eliminates the tracking requirements and reduces the shading effect [16], and thermal modelling was presented [17]. The use of phase change material (PCM) can enhance the productivity of solar stills up to 120% [18]. Further, the thermal performance of still can be enhanced by manipulating the thermo-physical peculiarities of water [3]. The use of nanoparticles is one of the effective heat transfer means to enhance the utilization of thermal energy in solar applications [19]. Nanofluids are eco-friendly in nature. Hence, it has attracted the attention of researchers over the world because of potential to enhance the thermo-physical characteristics such as specific heat, thermal conductivity, viscosity and density [4] compared to conventional fluids (water, glycols, alcohols, various oils, etc.). The heat transfer ability of base fluid can be enhanced due to enhanced thermo-physical characteristics [20]. Further, the plasmon resonance absorption band of metallic nanoparticles lies within the spectrum of infrared and visible region that enhances the optical and radiation absorption characteristic of base fluid [21].

Choi et al. [22] have conducted an analytical study on nanofluids and concluded that utilization of nanoparticles in base fluid enhances the heat transfer rate and thermal conductivity. Other experimental studies also represent the enhancement in thermal conductivity when nanoparticles were mixed in base fluid [23, 24]. Yu et al. [25] have reviewed the effect of parameter such as temperature, additives, particle volume concentration, particle material, particle size, particle shape and base fluid material on heat transfer rate and thermal conductivity. They have concluded that an enhancement of 15–40% in heat transfer was observed with the use of nanoparticle. Nguyen et al. [26] inspected the effect of nanoparticle size and temperature on viscosity of water nanofluid. Concentration, size and temperature of nanoparticle have a noteworthy impact on process of heat transfer [27]. The utilization of nanoparticles for enhancing the performance of solar–thermal devices has been prompted by several researchers [28–33]. Jani and Modi [3] deduced that the performance of solar energy-based thermal devices can be enhanced with the consumption of nanoparticles. Further, the use of nanoparticles enhances the heat transfer characteristics in wavy channel heat sink [34], in closed conduit [35] and in pool boiling [36]. Nanotechnology has been utilized for: (1) the blood flow analysis in medical sciences [37, 38]; (2) the entropy and exergy analysis of nanofluid under magnetic force in the porous medium [39]; (3) the analysis of electro-osmotic flow of Couette–Poiseuille nanofluids [40]; and (4) the analysis of bi-phase coupled stress fluid in the presence of Hafnium and metallic nanoparticles over an inclined plane [41].

Elango et al. [42] have analysed the performance of CSS with and without nanoparticles. In experiment, authors have utilized the different nanoparticles, namely iron oxide (Fe_2O_3), tin oxide (SnO_2), aluminium oxide (Al_2O_3) and zinc oxide (ZnO). 29.95% higher distillate was obtained for solar still with Al_2O_3 nanoparticles compared to the CSS. Kabeel et al. [43] have concluded that CSS with nanoparticles and an external arrangement of condenser enhance the productivity by 53.2% compared to the CSS. Omara et al. [44] have utilized Cu_2O and Al_2O_3 nanoparticles in corrugated wick-type CSS, and enhancement of 285.1% and 254.88% in yield was achieved than CSS. From analytical study, Sahota et al. [4] have developed the characteristic equation for passive-type double-sloped solar still using various nanoparticles and concentration. Authors have achieved enhancement in thermal efficiency of still (CuO—43.81%, TiO_2—46.10% and Al_2O_3—50.34%) with 0.25% nanoparticle concentration compared to base fluid. Sahota et al. [19] evolved the theoretical expression of fluid temperature for dual-slope solar still and analysed the performance for three different concentrations of Al_2O_3 nanoparticles (0.04%, 0.08% and 0.12%).

Modi et al. [45] have examined influence of concentration (0.2%, 0.1%, 0.05% and 0.01%) of Al_2O_3 nanoparticles on yield of DBSS. They observed that with a decrease in concentration of nanoparticles the output of still increases. 0.1% concentration of ZnO nanoparticles was utilized by Modi and Shukla [46] and Shukla and Modi [47] in hybrid solar still for enhancement in heat transfer, yield and regeneration of liquid desiccant $CaCl_2$ [46] and $MgCl_2$ [47]. The overall average efficiency is 22.77% [46] and 19.20% [47] for hybrid solar still. Nazari et al. [48] have conducted an experimental and analytical investigation on CSS augmented by means of Cu_2O nanoparticles and thermo-electric (TE) modules. The study found that inclusion of Cu_2O nanoparticles by 0.08% volume fraction in base fluid enhances the yield, energy and exergy efficiency by 82.4%, 81.5% and 92.6%, respectively. Further, the combined use of Cu_2O nanoparticles and TE channels enhance the yield, energy and exergy efficiency by 81%, 80.6% and 112.5%, respectively [49]. Rashidi et al. [50] have utilized the volume of fluid model for the theoretical study of impact of Al_2O_3 nanoparticles on productivity of CSS and achieved the enhancement of 25%.

Hence, the use of nanofluid in field of solar still can confer the new dimensions on performance of passive solar still. From the present literature, influence of nanoparticles has been studied on efficiency and productivity for CSS [48, 49]. However, significance of impact of different nanofluids with varying basin water depth has not been found for the SBDS solar still for the identification of higher-productive configuration. Moreover, the influence of orientation of SBDS solar still on performance is traceless in the present literature. These research gaps have been replete in the present study along with economic feasibility analysis.

The core objective of research is to investigate the influence of still orientation, water depth and different nanoparticles on productivity of SBDS solar stills. To execute the purpose, two identical SBDS solar stills were fabricated and the experiments were performed. In first set of experiments, productivity of still with 0.1% mass concentration of Al_2O_3 nanoparticles at various water depths (30 mm, 20 mm and 10 mm) was compared with the still without nanoparticles. The first set of experimentations were conducted for glass covers facing East–West and North–South directions at the location (20.61° N, 72.91° E). The second set of experiment were carried out for the still with and without 0.1% mass concentration of CuO nanoparticles at the 20 mm and 10 mm basin water depth and for the glass covers oriented towards North–South direction.

Solar still and experimental methodology

Fundamentals and heat exchange mechanism of SBDS solar still is depicted in Fig. 1. Solar still harnesses solar energy to obtain distilled water as a product. The saline water in basin of still is evaporated by absorbing incident solar radiations. The water vapour arises because of difference of temperature among the water and glass cover that came in contact with inner surface of glazing cover where it gets condensed. To collect the condensate, inclination is provided to glazing cover.

The basin of solar still has a shallow and wide structure to enhance the surface area. To increase the solar radiation absorption, black colour was painted on basin. The black painted basin raises the temperature of saline water that increases rate of evaporation. The transparent glass cover is utilized for condensation and to accumulate the distillate. Further, distilled yield from solar still increases with increase in temperature gap among the saline water and glass cover. The solar radiation transmitted from absorber plate is intercepted by glass cover, which generates greenhouse effect inside the still.

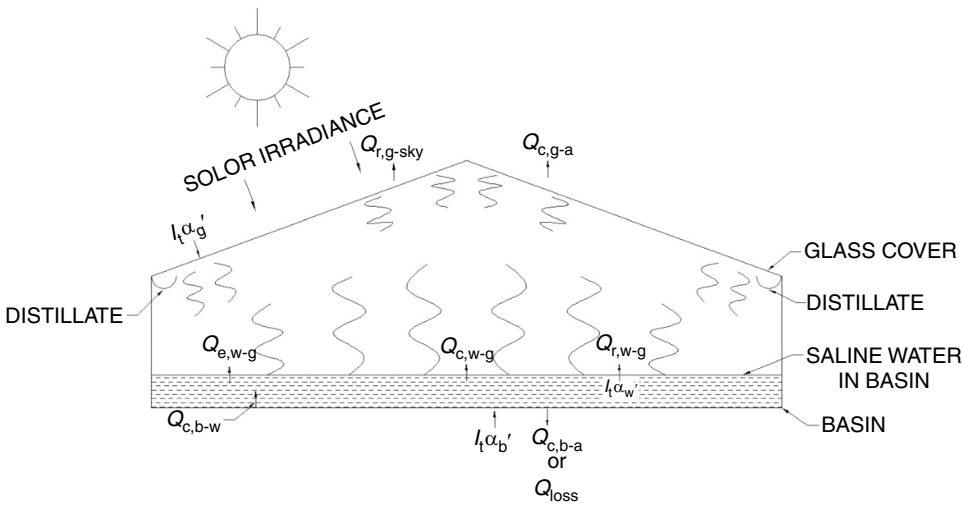

Fig. 1 Working principle and heat transfer mechanism of SBDS solar still

The solar radiations ($I_t \cdot \alpha_{b'}$) absorbed by the basin of solar still. From the basin, a part of heat is lost in environment (Q_{loss}) and a part of heat is supplied to saline water in basin ($Q_{c,b-w}$). The brackish water in basin gains the heat from basin ($Q_{c,b-w}$) and solar radiation ($I_t \cdot \alpha_{w'}$). The heat in brackish water leads to vaporization by means of evaporation ($Q_{e,w-g}$), convection ($Q_{c,w-g}$) and radiation ($Q_{r,w-g}$). The glass covers gain the heat from solar radiation ($I_t \cdot \alpha_{g'}$) and brackish water in basin ($Q_{e,lw-lg}, Q_{c,lw-lg}, Q_{r,lw-lg}$) and that heat is lost in the form of convection ($Q_{c,ug-a}$) and radiation ($Q_{r,ug-sky}$) in atmosphere.

Experimental model

The experimental model of SBDS solar still and wireframe model with elementary dimensions are depicted in Fig. 2a, b, respectively. The basin was fabricated from 2 mm thick sheet of galvanized iron (GI) with the size of 300 mm × 600 mm × 100 mm. To increase radiation absorption rate, basin was painted with black colour. To debilitate the heat transfer from the bottom and side walls of still, 10 mm thick plywood sheet (density ≈ 545 kg m^{-3} [51]) was utilized due to its low thermal conductivity (≈ 0.12 W m^{-1} K^{-1} [51]). The glass having 4 mm thickness was selected as glazing cover to capture and condense the evaporated water vapour. Semi-circular-shaped PVC pipe of 1 inch diameter was utilized to accumulate the distillate yield. To increase the solar radiations absorption and thermal conductivity, 0.1% concentration [42] of two nanoparticles such as Al_2O_3 and CuO was used with ground water as a base fluid. The reason for selection were: from literature, it has found that increment in thermal conductivity is higher for Al_2O_3 and CuO nanoparticles compared to other nanoparticles [52] and has high ability to disperse the heat in fluid [53].

In present work, glazing glass covers were tilted at an angle of 20° (≈ latitude of the location) on both sides at upper edge of the basin of solar still. The collecting channels were attached just below the glass cover to collect the distilled water. To supply makeup water and to attach temperature sensor inside basin, 10 mm diameter two holes were provided in side wall of basin. Silicon sealant was utilized to affix the glass. For drainage, 20 mm diameter hole was provided at bottom of basin. M-Seal was used to prevent the effusion from solar still.

Experimental methodology and instrumentation

For the study of impact of solar still orientation, water depth and different nanoparticles on distillate, two similar SBDS solar still and experimental set up were prepared as shown in Figs. 2b and 3, respectively. The experiments were conducted at location of (20.61° N, 72.91° E, elevation from mean sea level = 17 m) starting from 8:00 to 18:00 h.

In first set of experiments, productivity of still with 0.1% mass concentration of Al_2O_3 nanoparticles for 30 mm, 20 mm and 10 mm water depths in basin was compared with the still without nanofluid. The experimentations were conducted for glass covers oriented facing North–South and East–West directions. 0.1% mass concentration of nanoparticles have good stability (Zeta potential: − 52.3 mV) and the higher enhancement in thermal conductivity [42] as well as results in higher distillate output. Thus, 2.304 gm, 4.608 gm and 6.912 gm of Al_2O_3 nanoparticles were added to prepare the 0.1% concentrated nanofluid at water depth of 10 mm, 20 mm and 30 mm, respectively. Further, two-step method was used to prepare nanofluid without surfactant. Nanofluid was stirred 45 min in magnetic stirrer followed by ultrasonication using probe sonicator for 60 min. In second set of experiments, productivity of still with 0.1% mass concentration of CuO nanoparticles for 20 mm and 10 mm water depths in basin was compared to the still without nanoparticles. The experimentations were conducted for glass covers oriented facing North–South directions. Wind velocity, solar

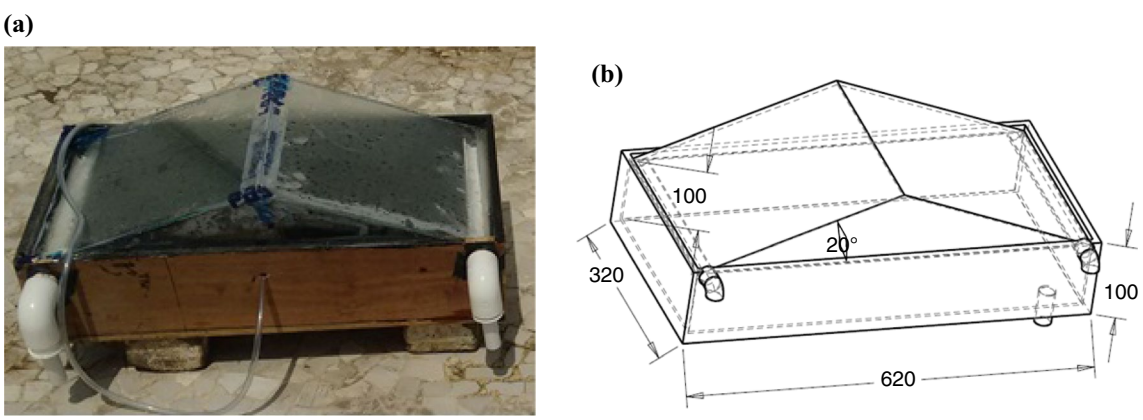

Fig. 2 **a** Actual fabricated model, **b** wireframe model of SBDS solar still (all dimensions are in mm)

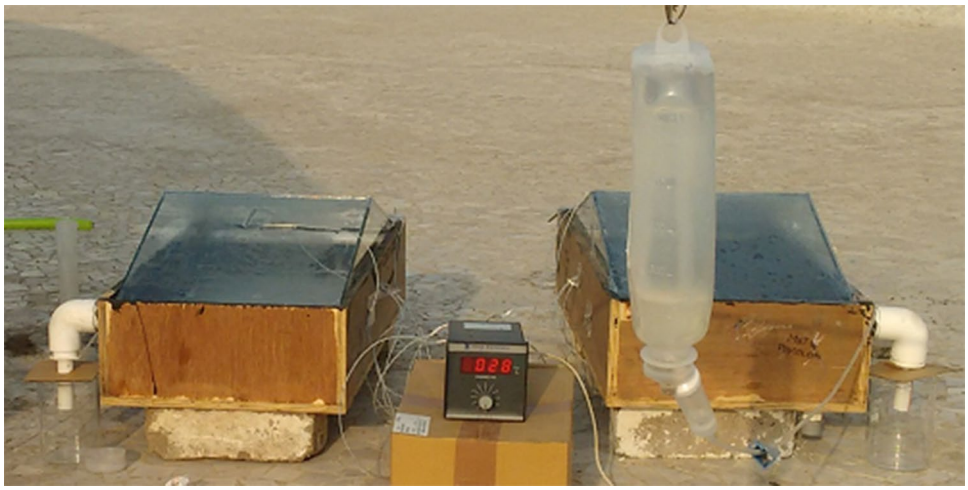

Fig. 3 Actual experimental set up

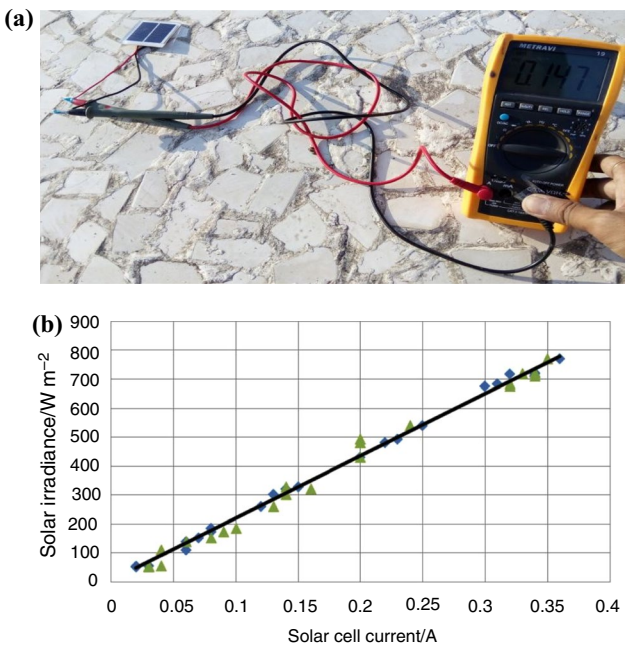

Fig. 4 **a** The measurement of solar radiation using calibrated solar PV cell. **b** Solar PV cell calibration curve

radiation, distilled output, atmospheric, glass cover, water and basin temperature were measured in experiments at an interval of 1 h for both solar still. The calibrated solar photovoltaic (PV) cell was utilized to measure solar radiation. As shown in Fig. 4a, solar radiations were recorded by keeping solar PV cell in short-circuiting mode on a horizontal surface. Figure 4b shows the calibration curve of the solar irradiation on horizontal surface recorded by pyranometer (W m^{-2}) versus solar cell current (amp). The solar radiations were calculated as: solar radiation (W m^{-2}) = cell current (amp) × 2175. The glass cover temperature, water temperature, basin temperature and atmospheric temperature were measured using PT-100 temperature sensors. The digital anemometer was utilized for measuring wind velocity, and measuring cylinders were used for measurement of distilled output. The total dissolved solids (TDS) and pH of ground water and distilled water were measured using TDS meter and pH meter.

The standard uncertainties of various instruments are presented in Table 1. Uncertainty is the probabilistic span of physical parameter within which the real values of physical parameters reside. In experiment, physical parameters were recorded using instruments, which has an inherent uncertainty known as accuracy of instruments. The standard uncertainty "*u*" was computed from [54, 55]:

Table 1 Instrumental uncertainty

Sr. no.	Device	Span	Accuracy	Standard uncertainty
1	Temperature sensor (PT 100)	0–400 °C	±0.1 °C	0.0577 °C
2	pH Meter	0–14 pH	±0.01 pH	0.0058 pH
3	Anemometer	0–45 m s^{-1}	±0.03 m s^{-1}	0.0173 m s^{-1}
4	TDS meter	0–99.9 ppm	±0.01 ppm	0.0058 ppm
5	Solar PV cell	0–2500 W m^{-2}	±1 W m^{-2}	0.5773 W m^{-2}
6	Measuring cylinder	0–100 mL	±1 mL	0.5773 mL

$$u = \frac{a}{\sqrt{3}}$$

where a = instrument accuracy. An accuracy of instrument was obtained from the data book of instruments.

Results and discussion

The first set of experiments were conducted to compare the total yield and efficiency of the still with 0.1% concentration of Al_2O_3 nanoparticles and the still without Al_2O_3 nanoparticles and with the glass covers facing North–South and East–West directions. The observations for the system parameters were recorded for 30 mm, 20 mm and 10 mm water depths in basin for both stills on hourly basis. The ground water had TDS of 740 ppm and pH of 6.5. After experiment, the TDS of 114 ppm and pH of 7.0 were obtained for distilled water.

For glass covers oriented towards North–South direction, Figs. 5a, 6a and 7a represent the hourly variation in glass cover, water, basin and ambient temperature of still without Al_2O_3 nanoparticles for 30 mm, 20 mm and 10 mm water depths, respectively, whereas Figs. 5b, 6b and 7b represent that for the still with 0.1% concentration of Al_2O_3 nanoparticles. From observations, the temperature of basin and water was achieved to be higher with the reduction of mass of water in basin for both the stills. Because of reduced mass of water at lower depth of water, temperature of various components of both the stills was obtained higher. Compared to the still without Al_2O_3 nanoparticles, temperature of glass cover, basin and water was achieved to be higher for the still with Al_2O_3 nanoparticles. Further, the temperature of water in solar still having Al_2O_3 nanoparticles remains higher than basin temperature. The reason was the use of nanoparticles enhances the energy storage capacity that absorb and store the higher amount of solar energy and delivers to the water in basin, which results in higher temperature of water. Further, the performance of still depends upon the temperature of various components of still and the heat transfer among the basin and water [3].

Figure 8a–c represents hourly change in solar radiations and comparison of distilled yield at water depth of 30 mm, 20 mm and 10 mm for the still with and without Al_2O_3 nanoparticles, respectively. The distillate output of 1120 mL m^{-2}, 1221 mL m^{-2} and 1252 mL m^{-2} at water depth of 30 mm, 20 mm and 10 mm was obtained from the still with nanoparticles, respectively, whereas distillate output for the still without nanoparticles was 938 mL m^{-2}, 950 mL m^{-2} and 989 mL m^{-2} for 30 mm, 20 mm and 10 mm water depths, respectively. Compared to the still without nanoparticles, higher yield of 19.40%, 28.53% and 26.59% was achieved from the still with nanoparticles at 30 mm,

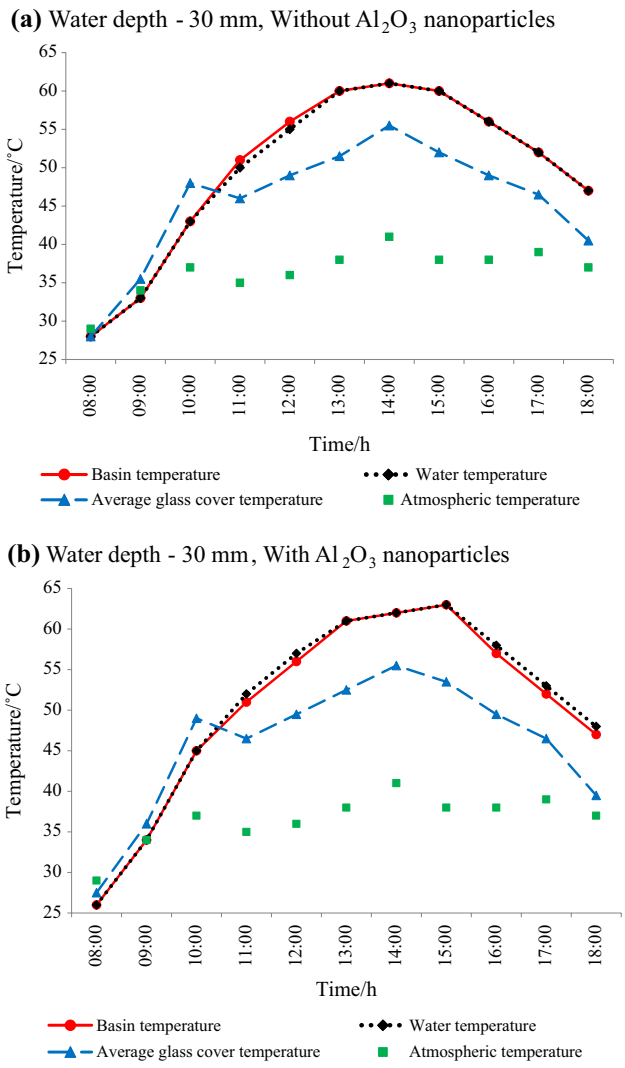

Fig. 5 Variation in temperatures for the still **a** without and **b** with Al_2O_3 nanoparticles and the glass covers oriented towards North–South direction (30 mm water depth)

20 mm and 10 mm water depths, respectively. The mixing of nanoparticles with water enhances the heat transfer characteristics and evaporative properties of mixture. Further, the addition of nanoparticles in water enhances the thermal conductivity and convective heat transfer coefficient of water. Therefore, ability of evaporation and condensation is improved in still with nanoparticles, resulting in enhancement of productivity. Compared to the still without Al_2O_3 nanoparticles, uniform and effective heat transfer occurs along the surface of water with the use of nanoparticles, which results in higher distillate output in the still with Al_2O_3 nanoparticles. Further, nanoparticles store the higher and excess amount of solar energy during the sunshine hours and that was liberated during the off-shine duration, which enhances the distillate output for the still with nanoparticles. Figure 9 shows the comparison of efficiency of the

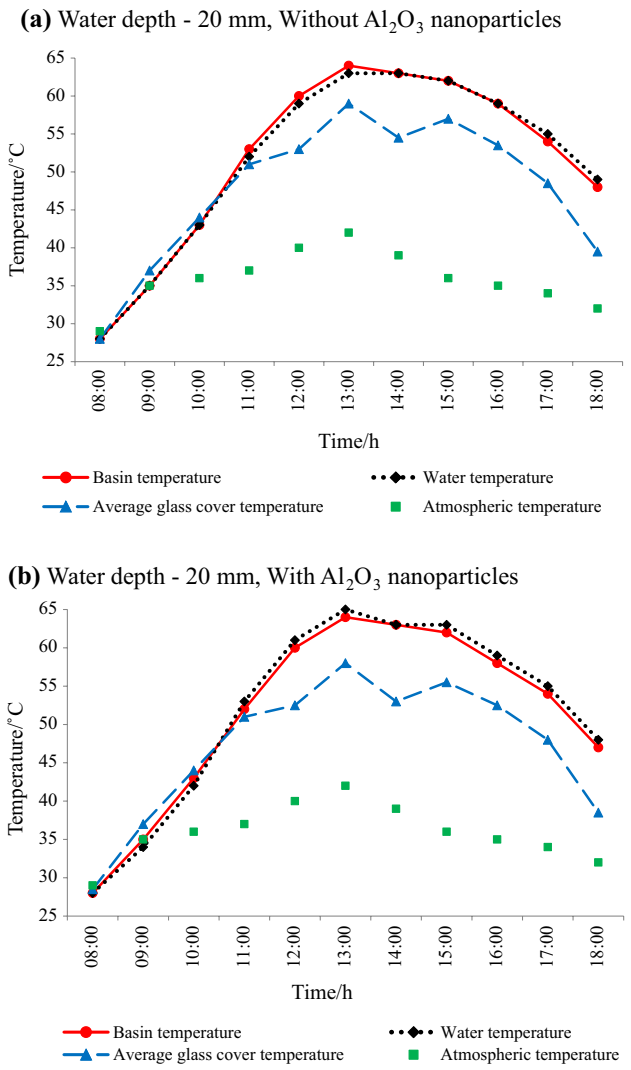

Fig. 6 Variation in temperatures for the still **a** without and **b** with Al_2O_3 nanoparticle and the glass covers oriented towards North–South direction (20 mm water depth)

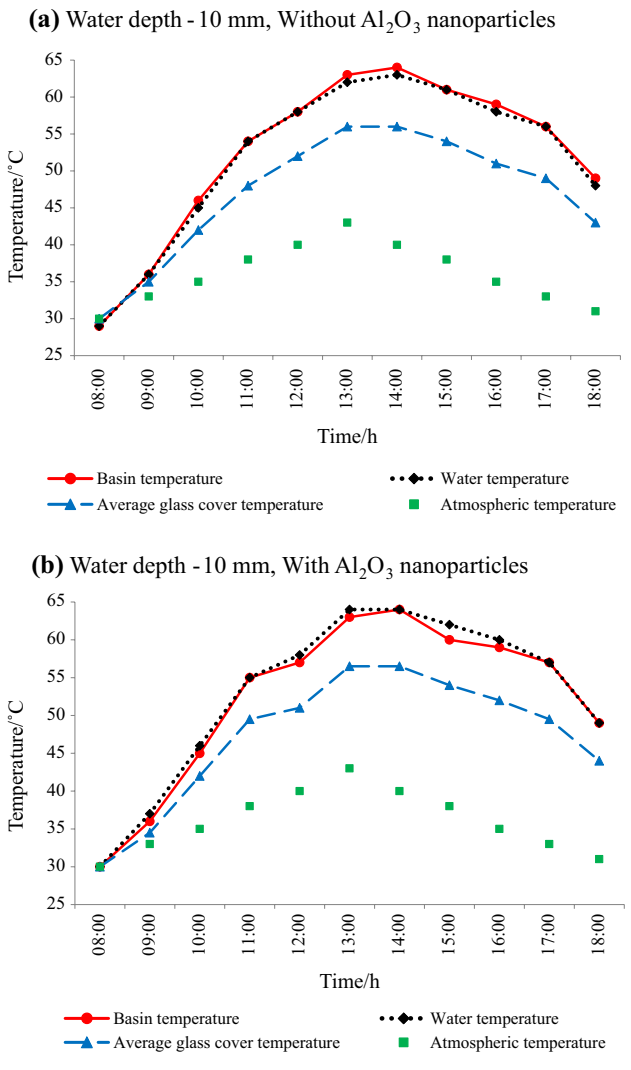

Fig. 7 Variation in temperatures for the still **a** without and **b** with Al_2O_3 nanoparticle and the glass covers oriented towards North–South direction (10 mm water depth)

still with and without nanoparticles at the water depth of 30 mm, 20 mm and 10 mm and for the glass covers oriented towards North–South directions. Compared to still without nanoparticles, an increment of 18.91%, 27.17% and 24.66% in efficiency was obtained for still with nanoparticles at the water depth of 30 mm, 20 mm and 10 mm, respectively.

For the glass covers facing East–West direction, Figs. 10a, 11a and 12a represent the hourly variation in glass cover, water, basin and ambient temperature of still without Al_2O_3 nanoparticles for 30 mm, 20 mm, 10 mm water depths, respectively, whereas Figs. 10b, 11b, 12b represent that for still with 0.1% concentration of Al_2O_3 nanoparticles. The trend observed for still with glass covers facing East–West direction was similar to the trend obtained in still with glass covers facing North–South direction. Figure 13a–c represents hourly change in solar radiations and comparison of distilled yield at water depth of 30 mm, 20 mm and 10 mm for still with and without Al_2O_3 nanoparticles, respectively. The distillate yield obtained from the still with nanoparticles was 1092 mL m^{-2}, 1080 mL m^{-2} and 1230 mL m^{-2} for the 30 mm, 20 mm and 10 mm water depth, respectively, whereas the distillate output from the still without nanoparticles was 914 mL m^{-2}, 933 mL m^{-2} and 967 mL m^{-2} for the 30 mm, 20 mm and 10 mm water depths, respectively. Compared to still without nanoparticles, higher yield of 19.48%, 15.76% and 27.20% was achieved from the still with nanoparticles at 30 mm, 20 mm and 10 mm water depths, respectively. Figure 14 shows the comparison of efficiency of the still with and without nanoparticles at the water depth of 30 mm, 20 mm and 10 mm and for the glass covers oriented towards East–West directions. Compared to still without nanoparticles, an increment of 19.44%, 15.24%

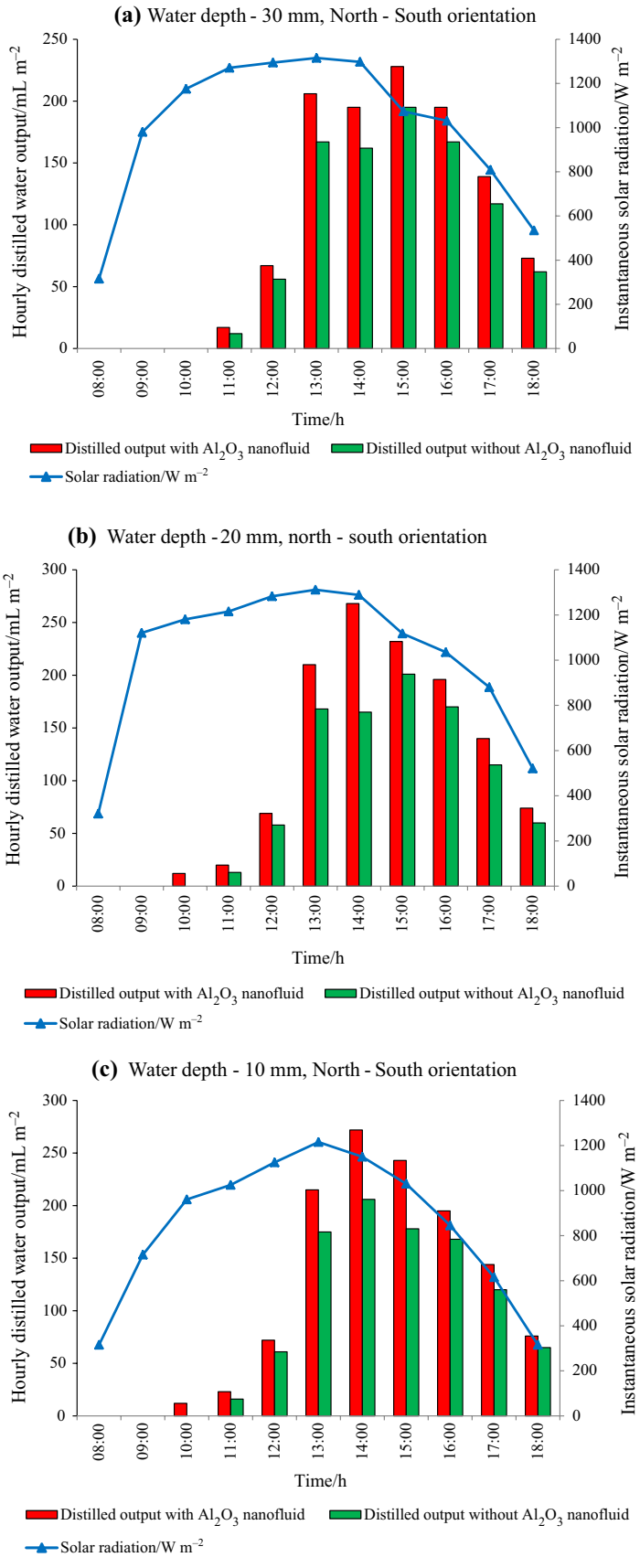

Fig. 8 Hourly variation in solar radiation and distillate yield for the still with and without Al_2O_3 nanoparticles and for the glass covers oriented towards North–South direction: **a** 30 mm, **b** 20 mm, **c** 10 mm water depths in basin

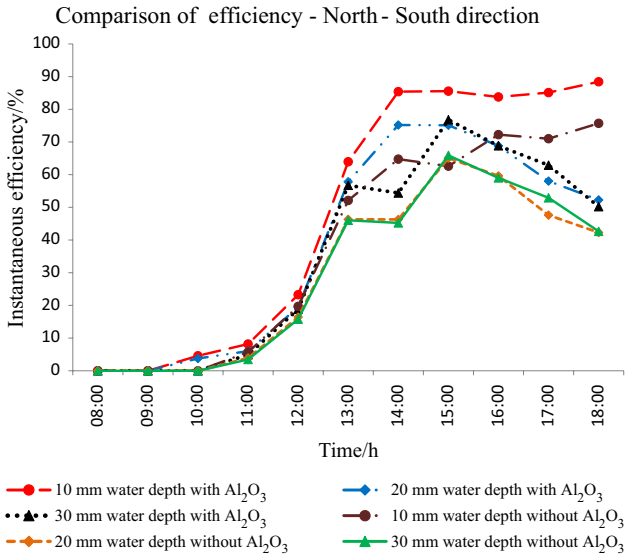

Fig. 9 Efficiency of the still with and without Al_2O_3 nanoparticles and the glass covers oriented towards North–South direction (30 mm, 20 mm and 10 mm water depths)

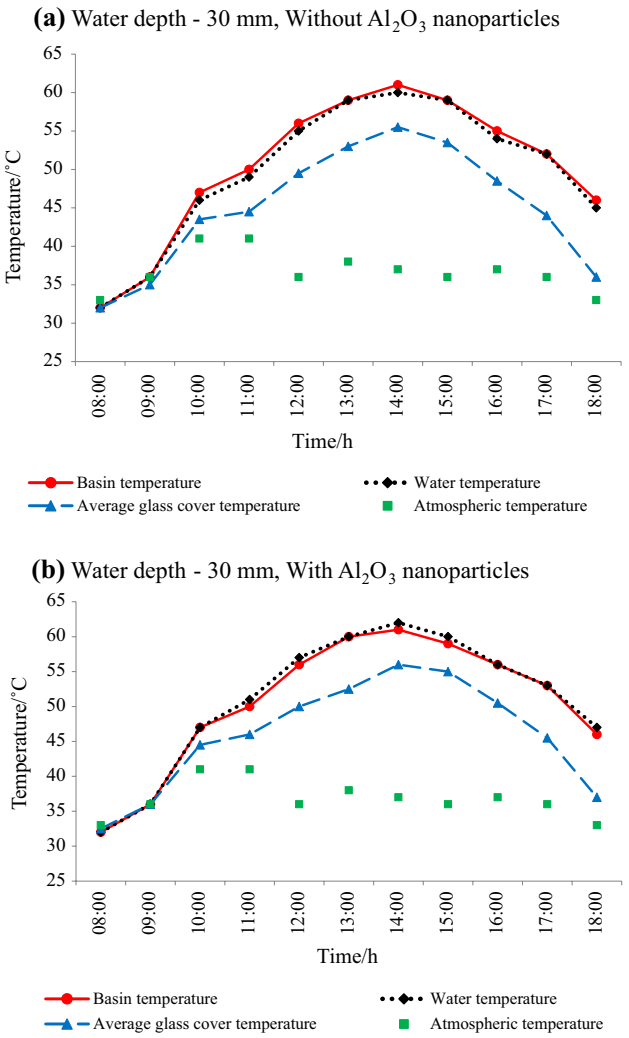

Fig. 10 Variation in temperatures for the still **a** without and **b** with Al_2O_3 nanoparticles and the glass covers oriented towards East–West direction (30 mm water depth)

and 23.25% in efficiency was obtained for still with nanoparticles at the water depth of 30 mm, 20 mm and 10 mm, respectively.

From first set of experiments, higher productivity and efficiency were obtained for the solar still with glass covers oriented towards North–South direction. Further, percentage increment in the distillate output and efficiency were observed higher at water depth of 20 mm and 10 mm compared to 30 mm in still with Al_2O_3 nanoparticles and for the glass covers oriented towards North–South direction. Therefore, the second set of experiments were conducted at water depth of 20 mm and 10 mm in basin with 0.1% concentration of CuO nanoparticles and without nanoparticles and for the glass covers oriented towards North–South directions.

Figures 15a and 16a represent the hourly variation in glass cover, water, basin and ambient temperature of the still without CuO nanoparticles for the 20 mm and 10 mm water depths, respectively, whereas the Figs. 15b and 16b represent that for the still with 0.1% concentration CuO nanoparticles. For second set of experiments, similar trend in variation of various temperatures has been found as observed in first set of experiments. Compared to still with Al_2O_3 nanoparticles, 77.31% rise in average temperature of water was achieved for the still with CuO nanoparticles at water depth of 10 mm and for glass covers oriented towards North–South direction. The reason may be: enhancement in thermal conductivity and heat transfer properties was higher in the still with CuO nanoparticles because of higher thermal conductivity of copper (Cu). Figure 17a, b represents the hourly variation of solar radiations and the comparison of distillate output at the water depth of 20 mm and 10 mm from the still with and without CuO nanoparticles, respectively. The distillate output obtained from the still with nanoparticles was 1554 mL m^{-2} and 1585 mL m^{-2} at the water depth of 20 mm and 10 mm, respectively, whereas distillate output for the still without nanoparticles was 982 mL m^{-2} and 1014 mL m^{-2} at the water depth of 20 mm and 10 mm, respectively. Thus, compared to still without CuO nanoparticles, higher yield of 58.25% and 56.31% was obtained at water depth of 20 mm and 10 mm for the still with nanoparticles, respectively. Compared to still without CuO nanoparticles, an increment of 65.99% and 50.70% in efficiency was obtained for still with nanoparticles at water depth of

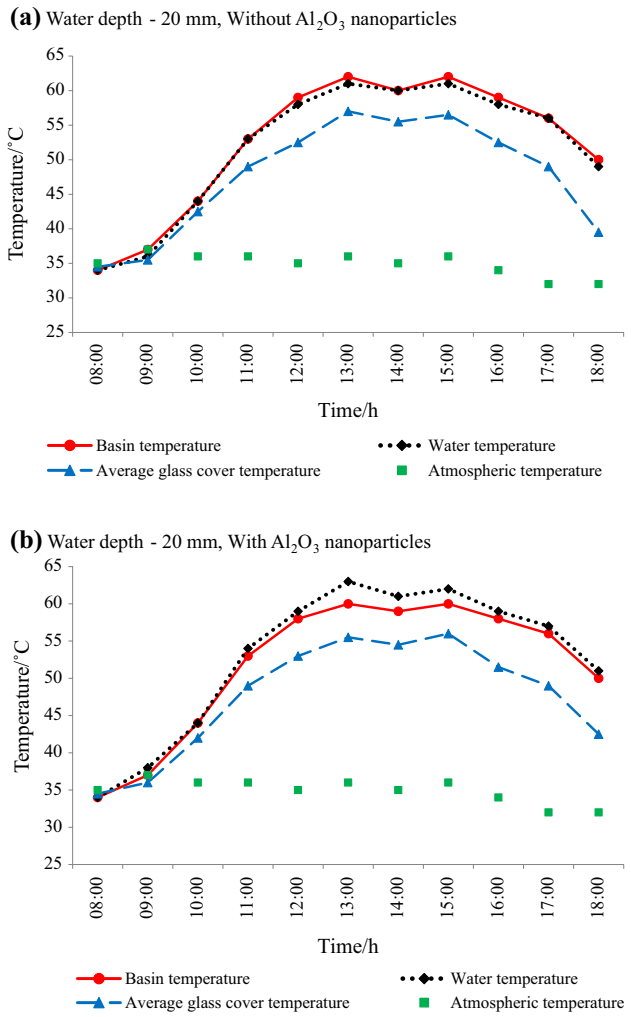

Fig. 11 Variation in temperatures for the still **a** without and **b** with Al_2O_3 nanoparticles and the glass covers oriented towards East–West direction (20 mm water depth)

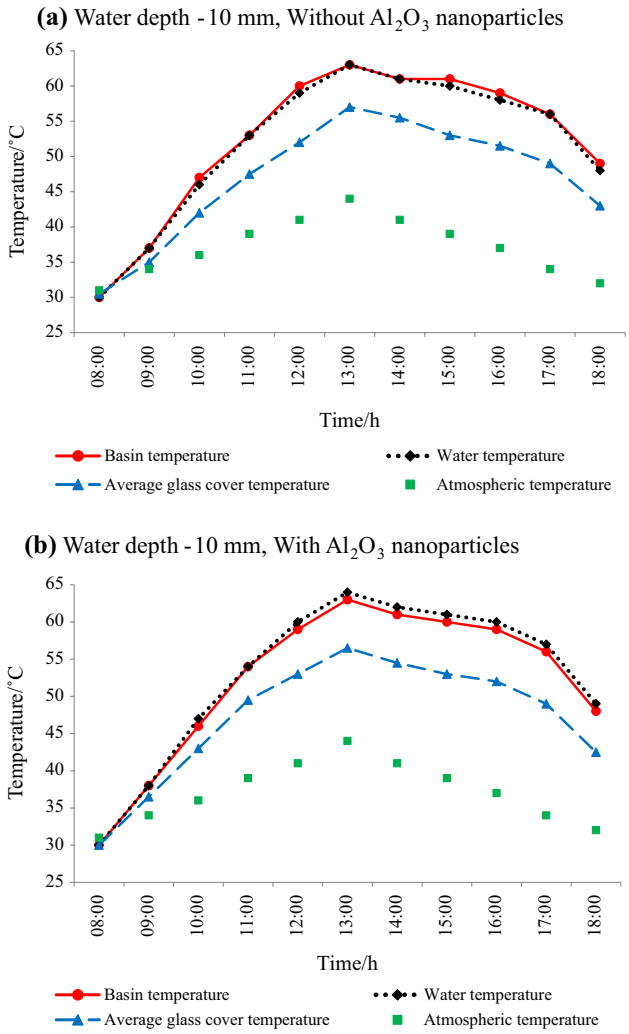

Fig. 12 Variation in temperatures for the still **a** without and **b** with Al_2O_3 nanoparticles and the glass covers oriented towards East–West direction (10 mm water depth)

20 mm and 10 mm, respectively. The distilled water yield obtained was higher at water depth of 10 mm than 20 mm, whereas increment in efficiency was obtained higher at water depth of 20 mm than 10 mm. Further, distillate output and efficiency for still with 0.1% concentration of CuO nanoparticles obtained were higher compared to the still with 0.1% concentration of Al_2O_3 nanoparticles.

Sahota and Tiwari [19] have studied the effect of various concentrations of Al_2O_3 nanoparticles on distillate yield obtained from passive-type SBDS solar still oriented towards East–West directions. From results, they have concluded that enhancement of 12.4% was observed in distillate output for 0.12% concentration of Al_2O_3 nanoparticles. Sahota and Tiwari [4, 56, 57] have studied the effect of various nanoparticles (Al_2O_3, TiO_2 and CuO) and concentration (0.2%, 0.25% and 0.3%) on distillate output for passive-type SBDS solar still oriented towards East–West directions. From theoretical study, monthly enhancement of 11.90% in distillate output was obtained for 0.25% concentration of Al_2O_3 nanoparticles at 35 kg mass of water in basin compared to CuO nanoparticles. Further, Sahota et al. [4, 56, 57] have theoretically achieved 13.50% enhancement in annual yield for SBDS still with the Al_2O_3 nanoparticles than the CuO nanoparticles and for the orientation of East–West direction, whereas in the present research work, daily increment of 27.27% and 26.60% at water depth of 20 mm and 10 mm was obtained with 0.1% concentration of CuO nanoparticles than Al_2O_3 nanoparticles and for the still orientation of North–South direction. Further, enhancement in yield observed in prior studies are: 54.22% for circular fin SBDS still compared to the square fin SBDS still at 10 mm water depth [12]; 18.3% for the jute cloth wick pile DBSS

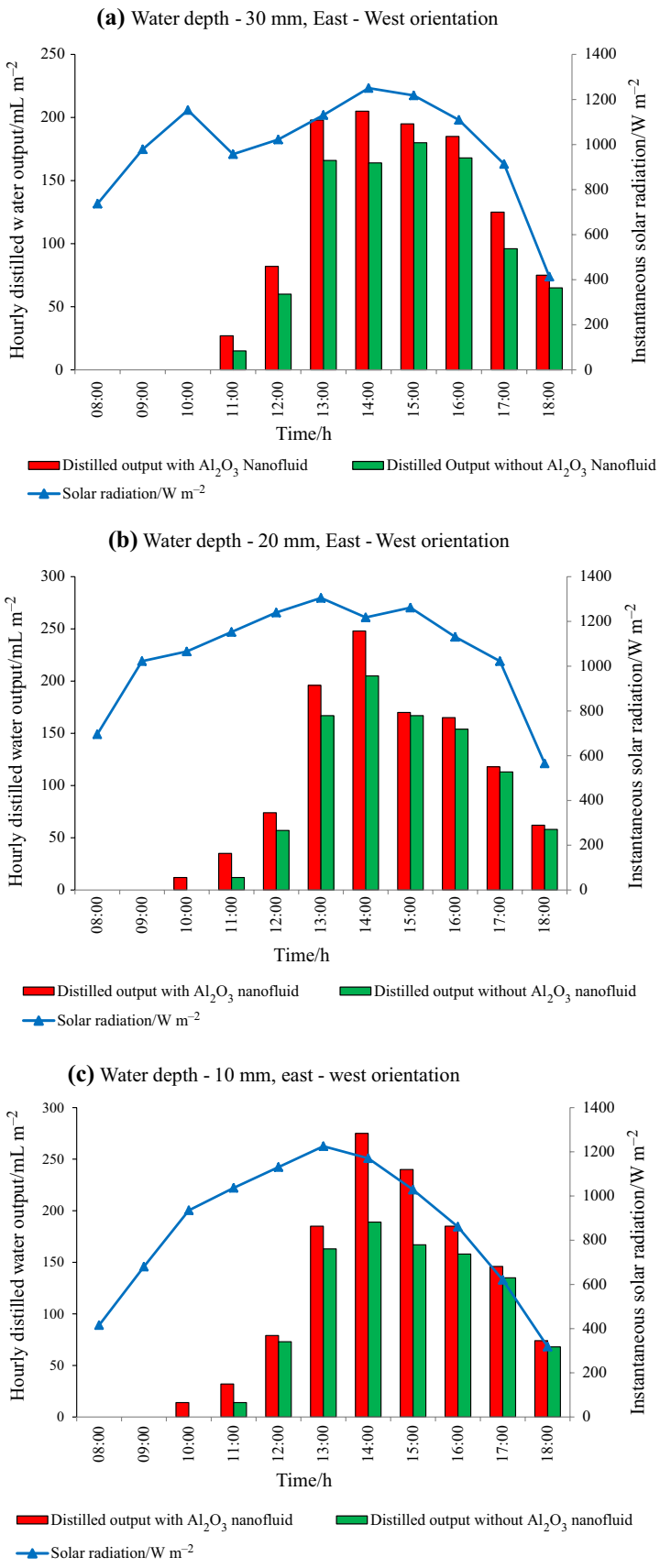

Fig. 13 Hourly variation in solar radiation and distillate yield for the still with and without Al_2O_3 nanoparticles and for the glass covers oriented towards East–West direction: **a** 30 mm, **b** 20 mm, **c** 10 mm water depths in basin

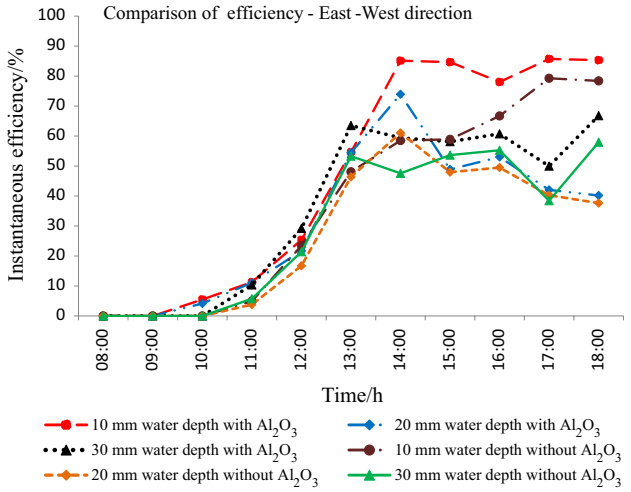

Fig. 14 Efficiency of the still with and without Al_2O_3 nanoparticles and the glass covers oriented towards East–West direction (30 mm, 20 mm and 10 mm water depths)

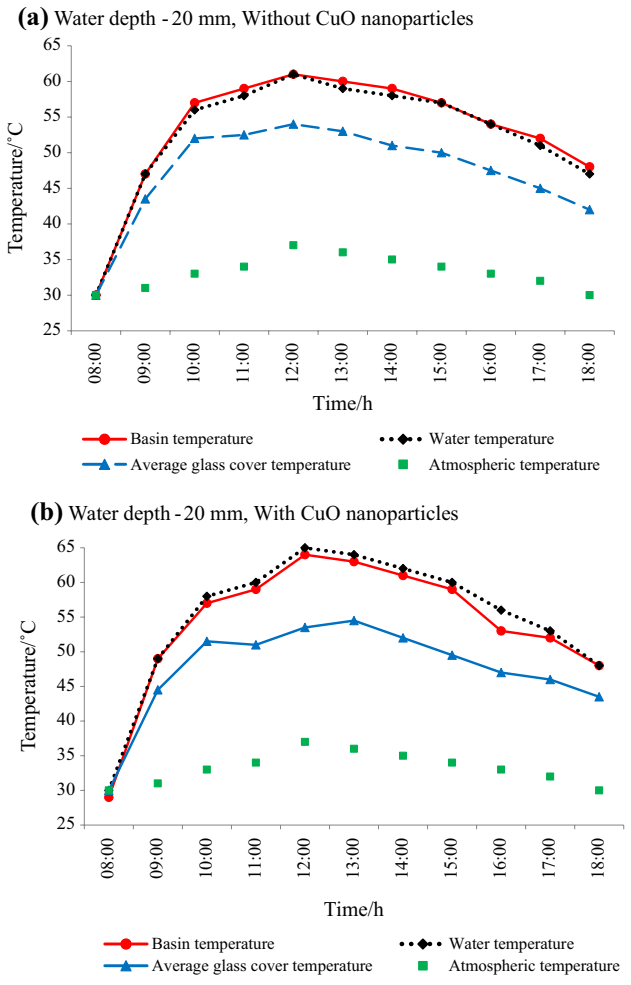

Fig. 15 Variation in temperatures for the still **a** without and with **b** CuO nanoparticles and the glass covers oriented towards North–South direction (20 mm water depth in basin)

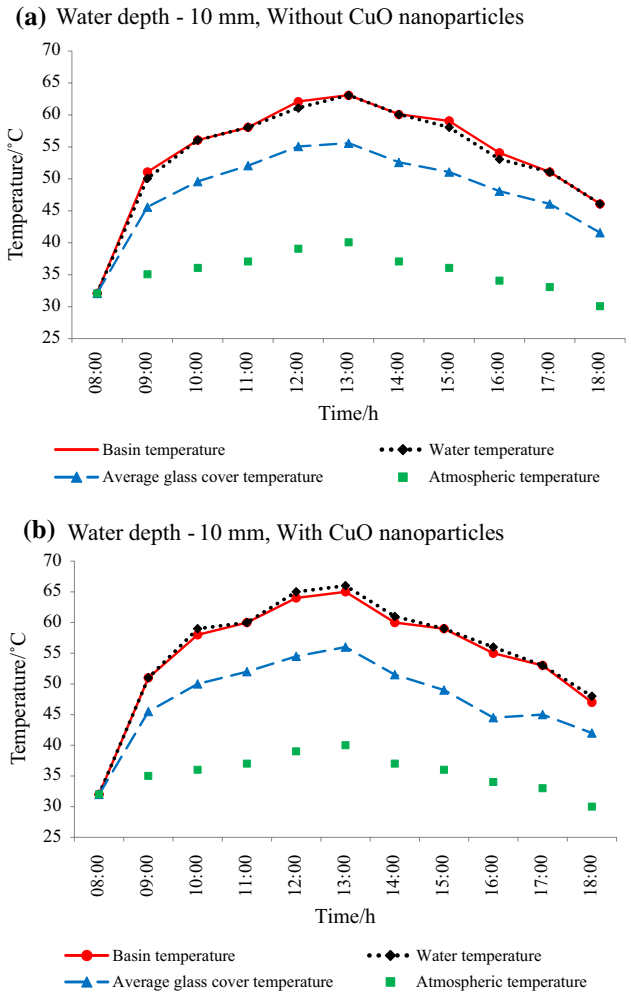

Fig. 16 Variation in temperatures for the still **a** without and with **b** CuO nanoparticles and the glass covers oriented towards North–South direction (10 mm water depth in basin)

still compared to the black cotton cloth wick pile DBSS still at the 10 mm water depth [11]; 45.8% for the square fin with wick CSS compared to the simple CSS [58]; and 21.5% with the corrugated CSS still compared to the simple CSS [59]. In present work, yield enhancement of 56.31% has been achieved for SBDS still with 0.1% concentration of CuO nanoparticles.

Economic analysis

The proposed configuration has to be economically viable for universally implemented on larger scale and for being accepted by the end users. Economics deals with the return obtained through the system on certain investment. For solar applications, cost plays an important role as it can be

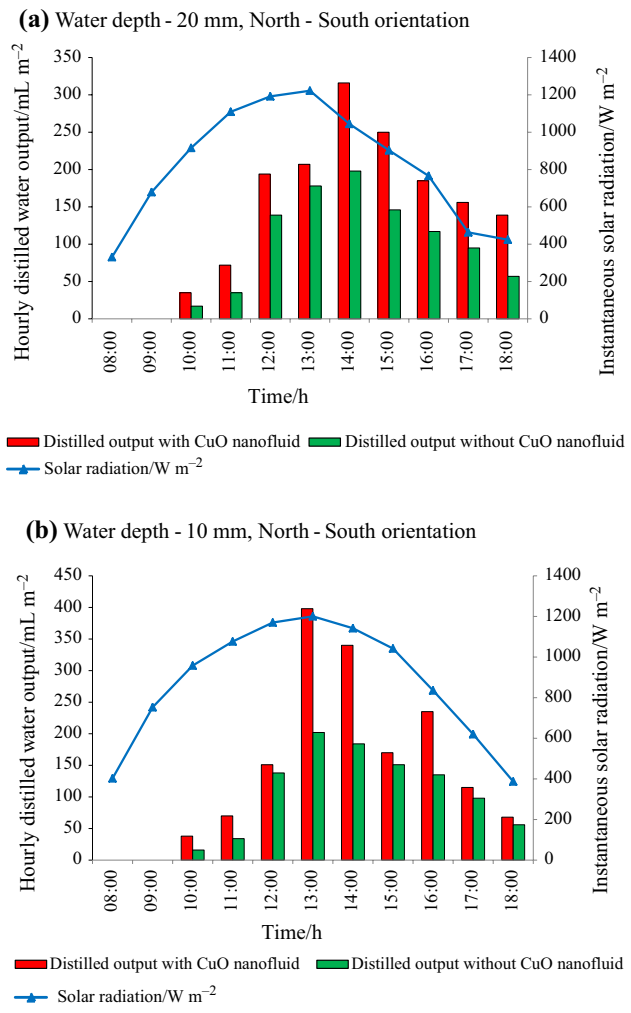

Fig. 17 Hourly variation in solar radiation and distillate yield for the still with and without CuO nanoparticles and the glass covers oriented towards North–South direction: **a** 20 mm, **b** 10 mm water depth in basin

exploited by the individual users as well as by the industrial organizations. Hence, economic analysis is the key factor in promoting use of solar–thermal applications. With the same aim, economic analysis of present desalination system has been performed.

The expenditure involved in fabrication of one SBDS solar still utilized in experiment is given in Table 2. The maximum yield of 1585 mL m^{-2} was achieved with the use of 0.1% concentrated CuO nanoparticle. The payback duration for system relies upon cost of saline water, construction cost and operation and maintenance cost. The costs of operation and maintenance and brackish water procurement are negligible. Considering average sunny days for location in a year as 250 days and cost of distilled water as ₹20/l,

Table 2 Fabrication expenditure of single solar still

Sr. no.	Narration of items	Expenses (₹)
1	GI sheet	500
2	Plywood	200
3	Fabrication cost	800
4	CuO nanoparticles cost	2000
5	Other expenditure	1000
	Total	4500

The payback duration

$$= \frac{\text{Capital Cost}}{\text{Average sunny days in experiment region} \times \text{Cash flow}}$$

$$= 4500/(250 \times 20 \times 1.585)$$

$$= 0.5678 \text{ year} \approx 208 \text{ days}$$

Conclusions

Authors have carried out the experimentations to study the impact of solar still orientation, water depths and different nanoparticles on yield of SBDS solar still. In study, two identical SBDS solar stills were developed and experiments were conducted at location (20.61° N, 72.91° E, Government Engineering College, Valsad). The first set of experiments were conducted to study the impact of 0.1% concentration of Al_2O_3 nanoparticles, still orientation (North–South direction and East–West direction) and water depths (30 mm, 20 mm and 10 mm) on the performance of SBDS solar still. For the still glass covers oriented towards North–South direction, higher yield of 19.40%, 28.53% and 26.59% was obtained at water depth of 30 mm, 20 mm and 10 mm for the still with nanoparticles, respectively, whereas higher yield of 19.48%, 15.76% and 27.20% was obtained at water depth of 30 mm, 20 mm and 10 mm water depth for the still with nanoparticles and for glass covers positioned facing East–West directions. Based on results of first set of experiments, second set of experiments were conducted to study the effect of 0.1% concentration of CuO nanoparticles and water depth (20 mm and 10 mm) on yield and for glass covers oriented towards North–South directions. An enhancement of 58.25% and 56.31% in distillate output was achieved at 20 mm and 10 mm water depths for the still with CuO nanoparticles, respectively, compared to the still without nanoparticles. Compared to still with 0.1% concentration of Al_2O_3 nanoparticles, higher distillate yield of 27.27% and 26.60% was obtained at 20 mm and 10 mm water depths for the still with 0.1% concentration of CuO nanoparticles and for glass covers oriented towards North–South directions.

Thus, the performance of SBDS still with CuO nanoparticles was achieved higher than the SBDS still with Al_2O_3 for the location.

References

1. Tiwari GN, Singh HN, Tripathi R. Present status of solar distillation. Sol Energy. 2003;75:367–73. https://doi.org/10.1016/j.solener.2003.07.005.
2. Shobha BS, Watwe V, Rajesh AM (2012) Performance evaluation of a solar still coupled to an evacuated tube collector type solar water heater. Int J Innov Eng Technol 1. ISSN 2319-1058.
3. Jani HK, Modi KV. A review on numerous means of enhancing heat transfer rate in solar-thermal based desalination devices. Renew Sustain Energy Rev. 2018;93:302–17. https://doi.org/10.1016/j.rser.2018.05.023.
4. Sahota L, Tiwari GN. Effect of nanofluids on the performance of passive double slope solar still: a comparative study using characteristic curve. Desalination. 2016;388:9–21. https://doi.org/10.1016/j.desal.2016.02.039.
5. Shukla DL, Modi KV. A technical review on regeneration of liquid desiccant using solar energy. Renew Sustain Energy Rev. 2017;78:517–29. https://doi.org/10.1016/j.rser.2017.04.103.
6. Muftah AF. Factors affecting basin type solar still productivity: a detailed review, Renew. Renew Sustain Energy Rev. 2014;32:430–47.
7. Xiao G, Wang X, Ni M, et al. A review on solar stills for brine desalination. Appl Energy. 2013;103:642–52. https://doi.org/10.1016/j.apenergy.2012.10.029.
8. Nafey AS, Abdelmotaliip M, Mabrouk AA. Parameters affecting solar still productivity. Energy Convers Manag. 2000;41:1791–809.
9. Kabeel AE, Khalil A, Omara ZM, Younes MM. Theoretical and experimental parametric study of modified stepped solar still. Desalination. 2012;289:12–20.
10. Modi KV, Ankoliya DB, Shukla DL. An approach to optimization of double basin single slope solar still water depth for maximum distilled water output. J Renew Sustain Energy. 2018;10:043708. https://doi.org/10.1063/1.5023088.
11. Modi KV, Modi JG. Performance of single-slope double-basin solar stills with small pile of wick materials. Appl Therm Eng. 2019. https://doi.org/10.1016/j.applthermaleng.2018.12.071.
12. Jani HK, Modi KV. Experimental performance evaluation of single basin dual slope solar still with circular and square cross-sectional hollow fins. Sol Energy. 2019;179:186–94. https://doi.org/10.1016/j.solener.2018.12.054.
13. Modi KV, Nayi KH, Sharma SS. Influence of water mass on the performance of spherical basin solar still integrated with parabolic reflector. Groundw Sustain Dev. 2020;10:100299. https://doi.org/10.1016/j.gsd.2019.100299.
14. Eibling JA, Talbert SG, Löf GOG. Solar stills for community use-digest of technology. Sol Energy. 1971;13:263–76. https://doi.org/10.1016/0038-092X(71)90007-7.
15. Elango C, Gunasekaran N, Sampathkumar K. Thermal models of solar still—a comprehensive review. Renew Sustain Energy Rev. 2015;47:856–911. https://doi.org/10.1016/j.rser.2015.03.054.
16. Nayi KH, Modi KV. Pyramid solar still: a comprehensive review. Renew Sustain Energy Rev. 2018;81:136–48. https://doi.org/10.1016/j.rser.2017.07.004.
17. Nayi KH, Modi KV. Thermal modeling of pyramid solar still. In: Solar desalination technology. Springer Singapore; 2019. p. 205–218
18. Omara AAM, Abuelnuor AAA, Mohammed HA, Khiadani M. Phase change materials (PCMs) for improving solar still productivity: a review. Berlin: Springer; 2019.
19. Sahota L, Tiwari GN. Effect of Al2O3 nanoparticles on the performance of passive double slope solar still. Sol Energy. 2016;130:260–72. https://doi.org/10.1016/j.solener.2016.02.018.
20. Solangi KH, Kazi SN, Luhur MR, et al. A comprehensive review of thermo-physical properties and convective heat transfer to nanofluids. Energy. 2015;89:1065–86. https://doi.org/10.1016/j.energy.2015.06.105.
21. Ravita D, Gamoz-Malgao LA, Rativa D, et al. Solar radiation absorption of nanofluids containing metallic nanoellipsoids. Sol Energy. 2015;118:419–25. https://doi.org/10.1016/j.solener.2015.05.048.
22. Xuan Y, Li Q. Investigation on convective heat transfer and flow features of nanofluids. J Heat Transf. 2003;125:151.
23. Xie H, Wang J, Xi T, et al. Thermal conductivity enhancement of suspensions containing nanosized alumina particles. J Appl Phys. 2002;91:4568–72. https://doi.org/10.1063/1.1454184.
24. Beck MP, Sun T, Teja AS. The thermal conductivity of alumina nanoparticles dispersed in ethylene glycol. Fluid Phase Equilib. 2007;260:275–8. https://doi.org/10.1016/j.fluid.2007.07.034.
25. Yu W, France DM, Routbort JL, Choi SUS. Review and comparison of nanofluid thermal conductivity and heat transfer enhancements. Heat Transf Eng. 2008;29:432–60. https://doi.org/10.1080/01457630701850851.
26. Nguyen CT, Desgranges F, Roy G, et al. Temperature and particle-size dependent viscosity data for water-based nanofluids—hysteresis phenomenon. Int J Heat Fluid Flow. 2007;28:1492–506. https://doi.org/10.1016/j.ijheatfluidflow.2007.02.004.
27. Dharmalingam R, Sivagnanaprabhu KK, Senthil Kumar B, Thirumalai R. Nano materials and nanofluids: an innovative technology study for new paradigms for technology enhancement. Procedia Eng. 2014;97:1434–41. https://doi.org/10.1016/j.proeng.2014.12.425.
28. Otanicar TP, Phelan PE, Golden JS. Optical properties of liquids for direct absorption solar thermal energy systems. Sol Energy. 2009;83:969–77. https://doi.org/10.1016/j.solener.2008.12.009.
29. Taylor RA, Phelan PE, Otanicar TP, et al. Nanofluid optical property characterization: towards efficient direct absorption solar collectors. Nanoscale Res Lett. 2011;6:1–11. https://doi.org/10.1186/1556-276X-6-225.
30. Nagarajan PK, Subramani J, Suyambazhahan S, Sathyamurthy R. Nanofluids for solar collector applications: a review. Energy Procedia. 2014;61:2416–34. https://doi.org/10.1016/j.egypro.2014.12.017.
31. Bozorgan N, Shafahi M. Performance evaluation of nanofluids in solar energy: a review of the recent literature. Micro Nano Syst Lett. 2015;3:5. https://doi.org/10.1186/s40486-015-0014-2.
32. Sajid Hossain M, Saidur R, Mohd Sabri MF, et al. Spotlight on available optical properties and models of nanofluids: a review. Renew Sustain Energy Rev. 2015;43:750–62. https://doi.org/10.1016/j.rser.2014.11.010.
33. Du M, Tang GH. Optical property of nanofluids with particle agglomeration. Sol Energy. 2015;122:864–72. https://doi.org/10.1016/j.solener.2015.10.009.
34. Sajid MU, Ali HM, Sufyan A, et al. Experimental investigation of TiO_2–water nanofluid flow and heat transfer inside wavy mini-channel heat sinks. J Therm Anal Calorim. 2019;137:1279–94. https://doi.org/10.1007/s10973-019-08043-9.
35. Abdelrazek AH, Kazi SN, Alawi OA, et al. Heat transfer and pressure drop investigation through pipe with different shapes using different types of nanofluids. J Therm Anal Calorim. 2019. https://doi.org/10.1007/s10973-019-08562-5.
36. Sarafraz MM, Pourmehran O, Yang B, et al. Pool boiling heat transfer characteristics of iron oxide nano-suspension under

constant magnetic field. Int J Therm Sci. 2020;147:106131. https://doi.org/10.1016/j.ijthermalsci.2019.106131.
37. Ellahi R, Zeeshan A, Hussain F, Asadollahi A. Peristaltic blood flow of couple stress fluid suspended with nanoparticles under the influence of chemical reaction and activation energy. Symmetry (Basel). 2019. https://doi.org/10.3390/SYM11020276.
38. Prakash J, Tripathi D, Triwari AK, et al. Peristaltic pumping of nanofluids through a tapered channel in a porous environment: applications in blood flow. Symmetry (Basel). 2019. https://doi.org/10.3390/sym11070868.
39. Sheikholeslami M, Ellahi R, Shafee A, Li Z. Numerical investigation for second law analysis of ferrofluid inside a porous semi annulus: an application of entropy generation and exergy loss. Int J Numer Methods Heat Fluid Flow. 2019;29:1079–102. https://doi.org/10.1108/HFF-10-2018-0606.
40. Ellahi R, Sait SM, Shehzad N, Mobin N. Numerical simulation and mathematical modeling of electro-osmotic Couette–Poiseuille flow of MHD power-law nanofluid with entropy generation. Symmetry (Basel). 2019. https://doi.org/10.3390/sym11081038.
41. Zeeshan A, Ellahi R, Mabood F, Hussain F. Numerical study on bi-phase coupled stress fluid in the presence of Hafnium and metallic nanoparticles over an inclined plane. Int J Numer Methods Heat Fluid Flow. 2019;29:2854–69. https://doi.org/10.1108/HFF-11-2018-0677.
42. Elango T, Kannan A, Kalidasa Murugavel K. Performance study on single basin single slope solar still with different water nanofluids. Desalination. 2015;360:45–51. https://doi.org/10.1016/j.desal.2015.01.004.
43. Kabeel AE, Omara ZM, Essa FA. Enhancement of modified solar still integrated with external condenser using nanofluids: an experimental approach. Energy Convers Manag. 2014;78:493–8. https://doi.org/10.1016/j.enconman.2013.11.013.
44. Omara ZM, Kabeel AE, Essa FA. Effect of using nanofluids and providing vacuum on the yield of corrugated wick solar still. Energy Convers Manag. 2015;103:965–72. https://doi.org/10.1016/j.enconman.2015.07.035.
45. Modi KV, Shukla DL, Ankoliya DB. A comparative performance study of double basin single slope solar still with and without using nanoparticles. J Sol Energy Eng. 2018;141:031008. https://doi.org/10.1115/1.4041838.
46. Modi KV, Shukla DL. Regeneration of liquid desiccant for solar air-conditioning and desalination using hybrid solar still. Energy Convers Manag. 2018;171:1598–616. https://doi.org/10.1016/j.enconman.2018.06.096.
47. Shukla DL, Modi KV. Hybrid solar still—liquid desiccant regenerator and water distillation system. Sol Energy. 2019;182:117–33. https://doi.org/10.1016/j.solener.2019.02.043.
48. Nazari S, Safarzadeh H, Bahiraei M. Experimental and analytical investigations of productivity, energy and exergy efficiency of a single slope solar still enhanced with thermoelectric channel and nanofluid. Renew Energy. 2019;135:729–44. https://doi.org/10.1016/j.renene.2018.12.059.
49. Nazari S, Safarzadeh H, Bahiraei M. Performance improvement of a single slope solar still by employing thermoelectric cooling channel and copper oxide nanofluid: an experimental study. J Clean Prod. 2018;208:1041–52. https://doi.org/10.1016/j.jclepro.2018.10.194.
50. Rashidi S, Akar S, Bovand M, Ellahi R. Volume of fluid model to simulate the nanofluid flow and entropy generation in a single slope solar still. Renew Energy. 2018;115:400–10. https://doi.org/10.1016/j.renene.2017.08.059.
51. Goss WP, Miller RG. Thermal properties of wood and wood products. In: Proceedings of thermal performance of the exterior envelopes of buildings. ASHRAE; 1992. p. 193–203.
52. Lee S, Choi SUS, Li S, Eastman JA. Measuring thermal conductivity of fluids containing oxide nanoparticles. Trans ASME J Heat Transf. 1999;121:280–9. https://doi.org/10.1115/1.2825978.
53. Das SK, Choi SUS, Patel HE. Heat transfer in nanofluids—a review. Heat Transf Eng. 2016;27:3–19. https://doi.org/10.1080/01457630600904593.
54. Kirkup L, Frenkel R. An introduction to uncertainty in measurement using the GUM (guide to the expression of uncertainty in measurement). 1st ed. Cambridge: Cambridge University Press; 2006.
55. Lira I (2002) Evaluation the measurement uncertainty fundamental and practical guidance. Institute of Physics Publishing.
56. Sahota L, Shyam Tiwari GN. Energy matrices, enviroeconomic and exergoeconomic analysis of passive double slope solar still with water based nanofluids. Desalination. 2017;409:66–79. https://doi.org/10.1016/j.desal.2017.01.012.
57. Sahota L, Tiwari GN. Exergoeconomic and enviroeconomic analyses of hybrid double slope solar still loaded with nanofluids. Energy Convers Manag. 2017;148:413–30. https://doi.org/10.1016/j.enconman.2017.05.068.
58. Rajaseenivasan T, Srithar K. Performance investigation on solar still with circular and square fins in basin with CO2 mitigation and economic analysis. Desalination. 2016;380:66–74. https://doi.org/10.1016/j.desal.2015.11.025.
59. Omara ZM, Hamed MH, Kabeel AE. Performance of finned and corrugated absorbers solar stills under Egyptian conditions. Desalination. 2011;277:281–7. https://doi.org/10.1016/j.desal.2011.04.042.